Nigerian Journal of Science and Environment 2025 Volume 23 (3) 20 – 44 ISSN: 3043 – 4440
https://doi.org/10.61448/njse233252

INVESTIGATION OF WETLAND AQUIFER IN AVIARA, DELTA STATE USING GEOPHYSICAL AND PUMPING TEST METHODS.

[1]Otheremu, O.P., Atakpo, [2]E.A.,[3]Ofomola, M.O. and [4]Avwenaghegha, J.O.

[1]Department of Physics, Southern Delta University Ozoro Delta State

Department of Physics, Delta State University Abraka Delta State

*Corresponding Author: Email:otheremuprecious@gmail.com (+234(0)8134364977]

ABSTRACT

This study investigates the wetland aquifer system in Aviara, Delta State, Nigeria. Vertical Electrical Sounding (VES), Electrical Resistivity Tomography (ERT), and Induced Polarization (IP) techniques using ABEM SAS 1000 Terrameter were applied to delineate subsurface layers and identify aquifer zones. Data were obtained from nine VES points and three ERT/IP transects using Schlumberger and dipole–dipole arrays. Interpretation was done using WinResist and Dipro software. The results showed that the subsurface consists of topsoil, clayey sand, fine sand, medium coarse sand, and coarse sand, with aquifers primarily found in sandy formations. Aquifer resistivity ranged from 904.4 to 2541.7 Ωm, while thickness varied from 15.4 to 29.9 m, suggesting favorable conditions for groundwater storage. Transmissivity values from VES ranged from 117.04 to 227.24 m²/day, with VES 8 showing the highest value. Hydraulic conductivity was consistently 7.6 m/day. Longitudinal conductance ranged from 0.0663 to 0.1984 S, indicating varying aquifer protective capacities. Groundwater electrical conductivity ranged from 17 to 46 µS/cm, suggesting fresh to moderately mineralized water. Porosity values ranged from 0.342–0.494% indicate highly porous formations. Pumping test results yielded a transmissivity of 131.04 m²/day, specific capacity of 0.497 m²/min, storativity of 36.24, and hydraulic conductivity of 7.6 m/day. ERT and IP results corroborated VES data, with high resistivity ranging from 165–5126 Ωm and low chargeability (<100 mV/V) marking permeable zones, while high chargeability indicated clayey layers. The findings provide essential insights for sustainable groundwater development and resource management in Aviara.wetland.

Key words: Aquifer Characterization; Vertical Electrical Sounding (VES); Electrical Resistivity Tomography (ERT); Induced Polarization; Pumping Test

INTRODUCTION

Wetlands are unique ecosystems characterized by seasonal or permanent water saturation, functioning as transitional zones between terrestrial and aquatic environments (Davidson *et al*., 2018). They typically occur where the water table is close to the land surface and are distinguished by slow-moving or standing water, waterlogged soils, and hydrophytic vegetation (Sánchez-Higueredo *et al.*, 2025). Found on every continent (Sharma and Naik, 2024), wetlands play critical hydrological and biogeochemical roles, such as nutrient retention and transformation, which help reduce eutrophication in connected water bodies (Griffiths and Mitsch, 2020; Emmanuel *et al.*, 2023). Their water balance is sustained by groundwater discharge, rivers, lakes, and tidal inflows, with seasonal fluctuations often leading to flooding and the development of anoxic soils (Keddy, 2010).

In Nigeria, particularly within the Niger Delta, wetlands are integral to the ecosystem and local livelihoods, supporting agriculture, fishing, and domestic water supply (Okonkwo *et al.*, 2015). They also provide vital ecosystem services, including flood control, sediment retention, and water purification. However, these benefits are increasingly undermined by anthropogenic pressures such as oil exploration, waste disposal, and urbanization, which degrade ecological integrity and threaten groundwater quality (Atakpo and Akpoborie, 2011; Newton *et al*., 2020). In Aviara, Delta State, such pressures have intensified concerns about the sustainability of groundwater resources.

Despite their significance, aquifers in Aviara wetlands remain poorly characterized, particularly with respect to subsurface lithology, hydraulic properties, and vulnerability to contamination. Previous studies in the Niger Delta often applied geophysical or hydrogeological techniques independently, with limited integration. As a result, knowledge of aquifer distribution, lithological structure, and hydraulic parameters remains inadequate, constraining the development of effective groundwater management strategies.

This study addresses the gap by integrating geophysical imaging techniques—Vertical Electrical Sounding (VES), Electrical Resistivity Tomography (ERT), and Induced Polarization (IP)—with hydrogeological testing through pumping methods (Ofomola *et al*.,2022; Anomohanran *et al.*, 2023; Emmanuel *et al.*, 2023) to investigate the wetland aquifer in Aviara, Delta State. The basis for integrating these techniques lies in their complementary strengths. VES provides one-dimensional depth sounding that estimates layer resistivity and thickness but lacks lateral resolution. ERT enhances this by producing two-dimensional subsurface images, which capture both lateral and vertical lithological variations. When combined with ERT, IP improves the ability to distinguish between saturated clay and water-bearing sandy formations. However, geophysical data remain indirect, requiring validation. Pumping tests therefore serve to ground-truth the interpretations by directly quantifying hydraulic parameters such as transmissivity and hydraulic conductivity. By combining these complementary approaches, the study provides a comprehensive characterization of wetland aquifers, thereby supporting sustainable groundwater use, ecosystem protection, and informed infrastructure planning in Aviara and similar environments.

MATERIALS AND METHODS

Location and Geology of the Study area

Aviara is located in the Isoko South Local Government Area of Delta State, Nigeria, within the geographical coordinates of Latitude 5°24'12''N and longitude 6°15'14''E. The terrain elevation above sea level is 17 meters. The town is situated within the lowland areas of the Niger Delta region, characterized by extensive wetlands, floodplains, and river networks (Nwankwoala and Okujagu, 2014). The community is predominantly agricultural, with farming and fishing serving as the main occupations. A significant proportion of the residents are engaged in subsistence agriculture, cultivating crops such as cassava, plantain, and yam, while fishing activities are carried out in the surrounding creeks and rivers. Members of the community are also involved in petty trading, craftwork, and public service, including employment in schools and health centers. With a distinct rainy season that usually lasts from March to October and a shorter dry season that lasts from November to February, Aviara has a humid tropical climate. According to Short and Stauble (1967), the study area consists of the mostly featureless Sombreiro-Warri Deltaic plain, flat to moderately undulating terrain, and gradual slopes toward the sea. The majority of freshwater wetlands are found close to riverbanks in low-lying areas. The three primary formations that make up its stratigraphy are Agbada, Akata, and Benin (Short and Stauble, 1967; Kouadio *et al*., 2020; Diab *et al.*, 2023). Formed during the Oligocene to Recent period, the Benin Formation represents the youngest unit, comprising predominantly coarse-grained floodplain sands and alluvial materials up to 2,000 meters thick (Eyankware and Ephraim, 2021). According to Ofomola *et al*., (2016), Holocene sediments connected to the deltaic plain and related wetlands frequently cover the Benin Formation.

Figure 1 shows the map of Delta State indicating the location of the study area while figure 2 shows data acquisition map of the study location.

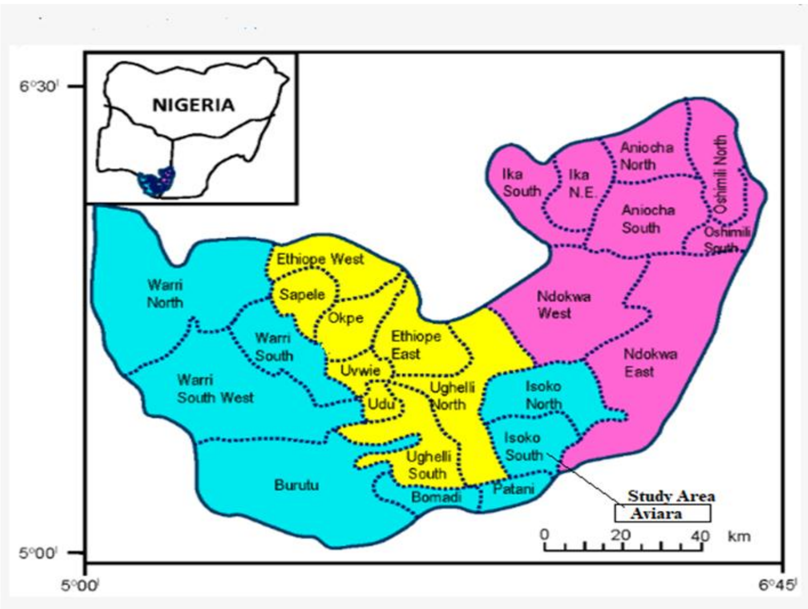

Figure 1: Map of Delta State indicating the location of the study area.

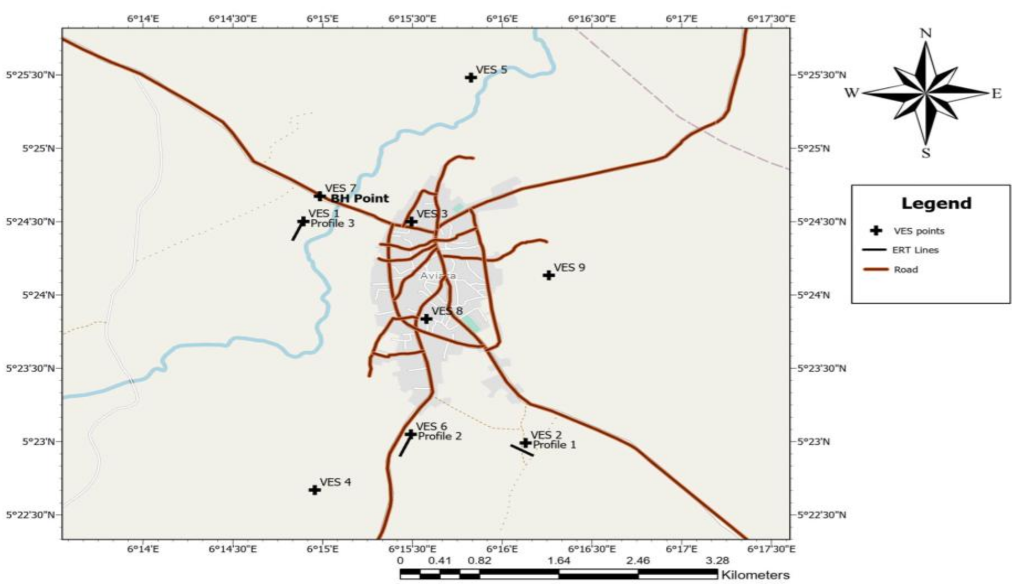

Figure 2: Data acquisition map of the study location

As observed in figure 2, Nine Vertical Electrical Sounding (VES) stations, labeled VES 1 to VES 9, are strategically positioned across the community to ensure adequate subsurface coverage. In addition to the VES points, three Electrical Resistivity Tomography (ERT) profiles were established, with Profile 1 located at VES 2, Profile 2 at VES 6, and Profile 3 at VES 1, to provide continuous subsurface imaging along selected transects. A borehole point is located close to VES 7, serving as a ground-truth control for correlating lithological information with geophysical results.

THEORETICAL BACKGROUND

Electrical resistivity methods are extensively employed to investigate a wide variety of geotechnical, geological, geophysical, environmental, and groundwater studies (Martinho, 2023). The fundamental objective of the resistivity method is to measure the electrical potential at the earth's surface resulting from the flow of electric current through the subsurface. This basic physical principle forms the foundation of surface electrical resistivity surveys. This fundamental principle is based on Ohm's Law which states that the resistance of a material is directly proportional to its cross sectional area, provided the materials temperature remain constant. This is mathematically represented in equation (1) below

$$R = \frac{\Delta V}{I} \qquad (1)$$

Where R is resistance, ΔV is potential difference and I is current. Two principal techniques within this method; Vertical Electrical Sounding (VES) and Electrical Resistivity Tomography (ERT) play significant roles in groundwater and environmental studies. VES is commonly employed to determine the vertical variation of subsurface resistivity, which helps in identifying aquifer layers and their thicknesses. In contrast, ERT provides two-dimensional or three-dimensional images of subsurface resistivity distribution, offering detailed insights into lithological variations, groundwater flow patterns, and potential contamination pathway.

Vertical Electrical Sounding

Vertical Electrical Sounding (VES) using the Schlumberger array was conducted at nine locations within the Aviara wetland to investigate subsurface lithology and delineate aquifer units. The Schlumberger array was adopted because of its suitability for layered subsurface investigations and efficiency in wetland terrain. The survey involved four electrodes: two outer current electrodes (A and B) and two inner potential electrodes (M and N). Current was introduced through A and B, while the potential difference was measured across M and N using ABEM SAS 1000 Terrameter. At the beginning of each sounding, the potential electrode separation (MN) was kept relatively small and constant. However, whenever the recorded potential difference decreased to a level that could compromise data accuracy, MN was expanded to improve measurement sensitivity. The current electrode separation (AB) was systematically increased in predetermined steps to achieve greater depth penetration. This sequence of AB expansions ensured consistent current penetration into deeper subsurface layers and minimized data distortion. VES points (from VES 1 to 9) were distributed to provide adequate spatial coverage of the wetland environment. Electrode expansion and data recording followed standard resistivity survey protocols to ensure data quality and repeatability. Figure 3 presents the Schlumberger electrode configuration adopted in the survey, highlighting the arrangement of current and potential electrodes used for resistivity measurements.

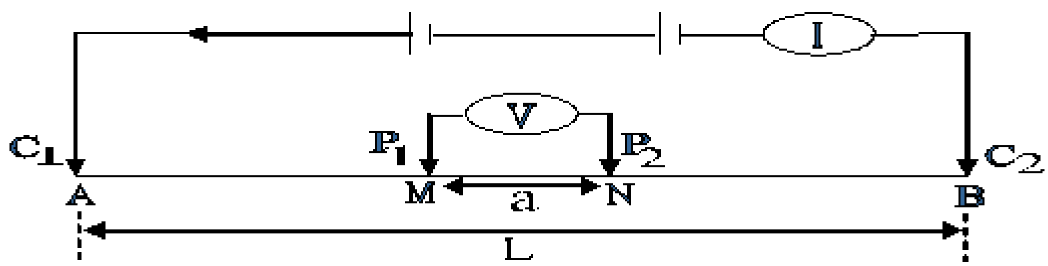

Figure. 3: A shematic representation of schlumberger electrodes configuration

The apparent resistivity

$\rho_a = \frac{\pi}{I}\Delta V \left[\frac{L^2 - a^2}{4^a} \right]$ (2)

where

ρ_a *is* apparent resistivity, ΔV is potential difference (V), I is current. The geometric factor K, specific to the Schlumberger array, was calculated using equation 3:

K$= \frac{\pi}{4}\left\{\left[\frac{L^2 - a^2}{a}\right]\right\}$ (3)

where

L = $\frac{AB}{2}$ is half the current electrode spacing

a = $\frac{MN}{2}$ is half the potential electrode spacing

To estimate layer resistivity and thickness, the bi-logarithmic plots of apparent resistivity versus electrode spacing were initially interpreted using partial curve matching with standard master and auxiliary curves (Akpan *et al*., 2013). These preliminary results were refined with WinResist software (Vander Velpen, 2004), which applied computer-aided inversion to enhance accuracy. The final interpretations were compared with borehole logs to verify subsurface stratigraphy and identify aquifer zones (ofomola *et al*.,2023).

Estimation of Aquifer Parameters from Vertical electrical Sounding

The aquifer parameters presented in Table 2 were derived from interpreted resistivity and thickness values using the following relations:

i. T = kh (4)

where K is hydraulic conductivity (m/day), h is aquifer thickness (m). Transmissivity expresses the capacity of the aquifer to transmit groundwater across its saturated thickness and is a key parameter in groundwater development.

ii. K = $\frac{T}{h}$ (5)

where K is hydraulic conductivity(m/day), T is transmissivity (m^2/day). This parameter represents the ease with which water can flow through the pore spaces or fractures of the aquifer under a unit hydraulic gradient. It is a fundamental indicator of aquifer productivity.

iii. S = $\sum_{i=1}^{n} \frac{h_i}{\rho_i}$ (6)

where S = Longitudinal Conductance, h_i = aquifer thicknesses, ρ_i = resitivities. Longitudinal conductance provides information on the protective capacity of overburden materials against infiltration of contaminants. Higher values generally indicate

Nigerian Journal of Science and Environment 2025 Volume 23 (3) 20 – 44 ISSN: 3043 – 4440
https://doi.org/10.61448/njse233252

better natural protection of underlying aquifers

iv. $R=\sum_{i=1}^{n} h_{i} \rho_i$ (7)

where h_i = aquifer thicknesses, ρ_i = resistivities, and R = transverse resistance.

Resistivity values were obtained from VES interpretation, while aquifer thicknesses were constrained using both VES results and available borehole information. These parameters collectively provide insights into aquifer geometry, protective capacity, and groundwater potential within the study area.

Electrical Resistivity Tomography

Electrical Resistivity Tomography (ERT) measurements were conducted to investigate the subsurface lithology and hydro geophysical conditions of the study area. The survey employed an ABEM SAS 1000 Terrameter using dipole dipole electrode configuration. This electrode configuration was selected due to its high sensitivity to lateral resistivity variations and suitability for delineating subsurface features with good horizontal resolution. Three parallel survey profiles were established, each with a total length of 100 m**.** Along each profile, 5 m electrode spacing was adopted, providing an optimal balance between investigation depth and data resolution. Stainless steel electrodes were inserted firmly into the ground to ensure good electrical contact. For each measurement, the ABEM SAS 1000 Terrameter injected a direct current into the ground through a pair of current electrodes, while the resulting potential difference was recorded between two separate potential electrodes. The data were processed using DIPRO WIN software to generate 2D resistivity models. GPS was used to record spatial coordinates, and all field measurements were precisely taken using a measuring tape.

Figure 4 provides a schematic illustration of the dipole–dipole electrode configuration applied in this study for both Electrical Resistivity Tomography (ERT) and Induced Polarization (IP) surveys. The arrangement highlights the positioning of current and potential dipoles along the survey line, which facilitated the acquisition of resistivity and chargeability data essential for subsurface characterization.

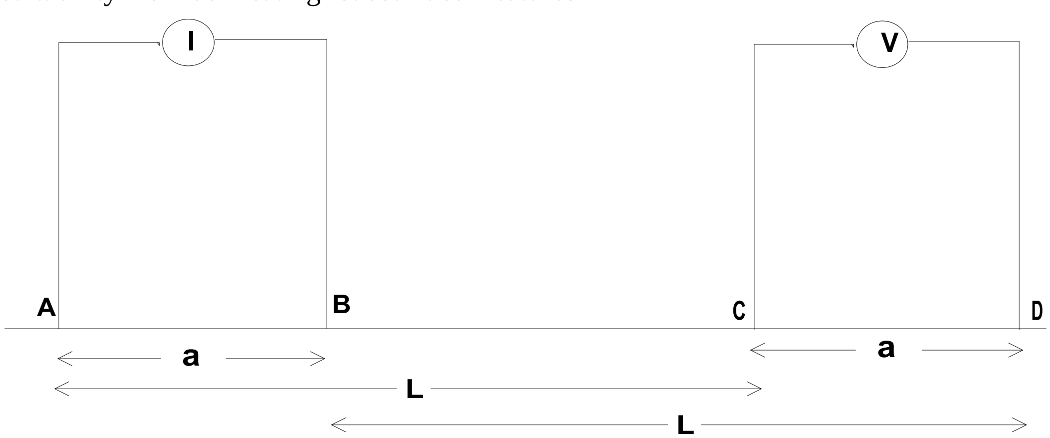

Figure. 4: A shematic representation of Dipole Dipole electrodes configuration

The apparent resistivity is represented by equation (4) giving by:

$$\rho_a = \frac{2\pi \nabla V}{I}\left\{\left[\frac{L^4 - a^2 L^2}{2a^2 L}\right]\right\} \quad (8)$$

Hence $\rho_a = \frac{K \nabla V}{I}$ (9)

Nigerian Journal of Science and Environment 2025 Volume 23 (3) 20 – 44 ISSN: 3043 – 4440
https://doi.org/10.61448/njse233252

where $K = \frac{\pi}{a}\left\{\left[\frac{L^2-a^2L}{a}\right]\right\}$ is the geometric factor for the dipole-dipole configuration ρ_a is the apparent resistivity, a is the electrode spacing, and π is a constant equivalent to 3.142, ΔV is the potential difference, I is the current injected.

Induced Polarization

Induced Polarization (IP) surveys were conducted using an ABEM SAS 1000 Terrameter in a dipole–dipole configuration to map subsurface chargeability variations across the study area. Current was introduced into the ground through paired current electrodes, and the resulting potential difference was measured at corresponding potential electrodes along the survey lines. Three profiles, each 100 m long with an electrode spacing of 5 m, were surveyed. Time-domain IP measurements were recorded, and chargeability values were expressed in millivolts per volt (mV/V). The chargeability (M) was computed using the time-domain formula in equation 10:

$$M = \frac{1}{V_0}\int_{t_i}^{t_{i+1}} V(t)\partial t \qquad (10)$$

Where $V(t)$ is the decaying voltage, t_i *and* t_{i+1} is the start and stop time of the interval and V_0 is the voltage measured before the current is turned off. The chargeability data, when integrated with resistivity results, were applied to delineate lithological variations, clay content, and potential aquifer development zones within the study area.

Pumping Test

The pumping test was carried out to evaluate the capacity of existing borehole and to determine the hydraulic characteristics or parameters of the aquifers, which are essential for groundwater development, management, in the wetland environment. Specifically, the test provided field-based estimates of transmissivity, hydraulic conductivity, storativity, and specific yield, which complement the geophysical interpretations. A constant-rate single-well pumping test was conducted on already existing borehole within the study area. The static water level was first measured prior to pumping. Pumping was then carried out at a constant discharge rate of 0.179 m^3/min for a duration of 200 mins. Drawdown in the pumping well was monitored at predetermined time intervals using a water level indicator. Following the pumping phase, recovery of the water level was also observed until near-static conditions were reached.

The drawdown data were analyzed using the Cooper–Jacob straight-line method (Gomo, 2019; Anomohanran *et al*., 2021; Azffri *et al*., 2022). This method, a late-time approximation of the Theis solution, was considered appropriate because the aquifers in the study area are predominantly unconfined to semi-confined (Jiao and Rushton, 1995; Kruseman and de Ridder, 2000; Anomohanran and Iserhien-Emekeme, 2014). However, observation distances were relatively close to the pumping wells and drawdowns were moderate, thereby minimizing delayed-yield effects that often complicate unconfined aquifer tests. Under these conditions, the Cooper–Jacob approach is suitable for estimating aquifer parameters. Aquifer properties, including transmissivity, hydraulic conductivity, storativity, and specific yield, were subsequently determined from the Cooper–Jacob analysis using Equations (11)–(14).

Equation 11 denotes the transmissivity (T) of the aquifer which expresses its ability to transmit water through the entire saturated thickness. It is determined from the slope of the drawdown–time plot using the Cooper–Jacob method and incorporates the constant pumping rate (Q) and the slope of the straight-line portion of the drawdown curve (ΔS). It is given by:

Nigerian Journal of Science and Environment 2025 Volume 23 (3) 20 – 44 ISSN: 3043 – 4440
https://doi.org/10.61448/njse233252

$$T = \frac{2.3\,Q}{4\pi \times \Delta S} \quad (11)$$

Equation (12) represents the storativity (S), a dimensionless parameter that describes the volume of water an aquifer can release or store per unit surface area per unit decline in hydraulic head. It is derived from the time of pumping (t_0) on the drawdown–time curve, the transmissivity (*T*), and the radial distance (*r*).

$$S = \frac{2.3\,Tt_0}{r^2} \quad (12)$$

Equation (13) gives the specific yield (Sy), which is the fraction of groundwater that drains freely under the influence of gravity in an unconfined aquifer. It is expressed as the ratio of the pumping rate (*Q*) to the slope of the drawdown curve (*ΔS*).

$$Sy = \frac{Q}{\Delta S} \quad (13)$$

Finally, Equation (14) defines the hydraulic conductivity (K) of the aquifer, which measures the ease with which water can move through the pore spaces or fractures of the aquifer material. It is obtained by dividing the transmissivity (*T*) by the aquifer thickness (*b*). it is given by:

$$K = \frac{T}{b} \quad (14)$$

Hence, these equations provide a quantitative basis for evaluating the aquifer's capacity, storage properties, and hydraulic behavior of the Aviara wetland.

Formation Factor

The formation factor is a dimensionless parameter that quantifies the relationship between the bulk resistivity of a rock saturated with a conductive fluid and the resistivity of the fluid itself (Amakiri, *et al*; 2024). The electrical formation factor was determined from the modeled field resistivity data using the expression proposed by Archie (1942) using equation 15:

$$F = \frac{p_b}{p_w} = a\,\emptyset^{-m} \quad (15)$$

In this expression, 'a' denotes the pore geometry factor, a lithology dependent coefficient that typically ranges between 0.5 and 1.5. The parameter p_w represents the resistivity of the pore water, while p_b corresponds to the bulk resistivity of the aquifer. The symbol $\emptyset$ refers to porosity, and 'm' is the cementation factor, which reflects the degree of compaction and grain arrangement within the formation."

For a given porosity, it can be qualitatively observed that the formation factor tends to increase as the sand becomes more cemented. It has a minimum value of unity when the bulk resistivity equals the resistivity of the saturating water, which corresponds to a porosity of one, and it gradually increases as the porosity decreases.

To evaluate the formation factor, we used bulk resistivity (ρb) values, obtained from the 1-D resistivity inversion while the measured pore water resistivity (ρw) values were obtained from borehole situated in close proximity to each Vertical Electrical Sounding (VES) station, resulting in a total of nine representative samples for analysis. In order to maintain the integrity of the results, electrical conductivity (EC) measurements were carried out directly at the sampling locations, to avoid any alteration in the water's physicochemical properties that could occur during transportation or storage. The EC value of each sample was recorded in micro siemens per centimeter (µS/cm). To derive the specific resistivity of the pore water, the reciprocal of each measured EC value was calculated. This parameter is important for understanding the ionic content and mineralization levels of the groundwater, which in turn influence aquifer quality and suitability for various uses.

Porosity

The porosity of the aquifer was estimated from the Vertical Electrical Sounding (VES) results using the modified Archie's equation, which relates the bulk resistivity of a saturated formation to its porosity, fluid resistivity, and cementation factor (Archie, 1942). The equation is expressed as:

$$\emptyset = (\frac{a}{F})^{1/m} \quad (16)$$

where $\emptyset$ is porosity, F is formation factor, a is pore geometry (coefficient of lithology) which is an empirical constant (default = 1), m is cementation exponent ((default = 2). The resulting porosities are shown in Table 3.

RESULTS AND DISCUSSION

Figures 5, 6 and 7 show the Vertical Electrical Sounding (VES) curve obtained from VES 1, VES 2, and VES 5. The curves depict the interpreted geoelectric parameters, including the number of subsurface layers, their resistivity values, thicknesses, and corresponding depths. This information provides a basis for understanding the lithological sequence and groundwater-bearing formations at the site.

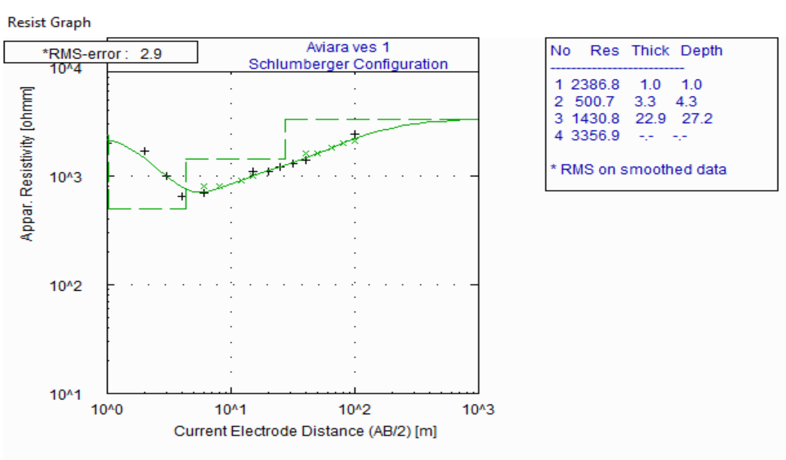

Figure 5: Vertical Electrical Sounding curves obtained from VES 1

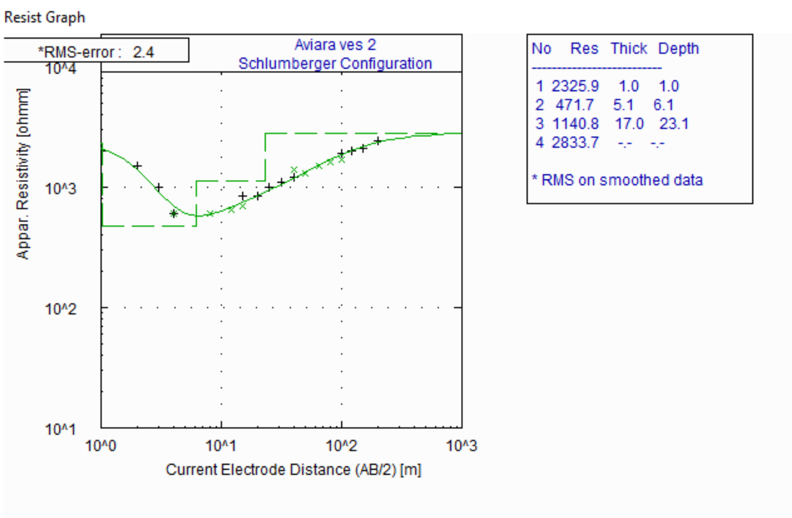

Figure 6: Vertical Electrical Sounding curves obtained from VES 2

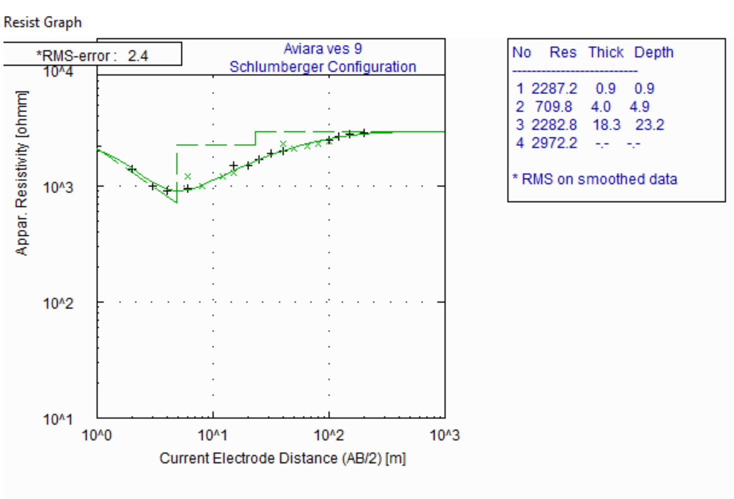

Figure 7: Vertical Electrical Sounding curves obtained from VES 9

Table 1 presents the computer iterated results obtained from the interpretation of the Vertical Electrical Sounding (VES) data. The results include the number of layers, their corresponding resistivity values, thicknesses, and depths, which provide essential information for delineating the subsurface lithology and evaluating aquifer potential within the study area.

Table 1: Computer Iterated Results

VES Number	Layer	Resitivity (Ωm)	Thickness (m)	Depth (m)	Curve type	Lithology
VES 1	1	2386.8	1.0	1.0	HA	Top soil
	2	500.7	3.3	4.3		Fine sand
	3	1430.8	22.9	27.2		Medium coarse sand
	4	3356.9				Coarse Sand
VES 2	1	2325.9	1.0	1.0	HA	Top soil
	2	471.7	5.1	6.1		Clayey Sand
	3	1140.8	17.0	23.1		Medium coarse Sand
	4	2833.7				Coarse Sand
VES 3	1	1830.0	0.6	0.6	HA	Top soil
	2	407.8	2.9	3.5		Clayey Sand
	3	904.4	17.4	20.9		Fine Sand
	4	2071.9				Coarse Sand
VES 4	1	2314.5	0.8	0.8	HA	Top Soil
	2	590.8	4.0	4.8		Fine Sand
	3	1530.0	18.9	23.7		Medium Coarse Sand
	4	3345.8				Coarse Sand
VES 5	1	2192.4	1.0	1.0	HA	Top soil
	2	534.1	3.4	4.5		Fine Sand
	3	1472.6	18.3	22.8		Medium Coarse Sand
	4	3466.3				Coarse Sand
VES 6	1	2136.0	0.8	0.8	HA	Top Soil
	2	884.4	5.9	6.7		Fine Sand
	3	2323.0	15.4	22.1		Medium Coarse Sand
	4	3740.0				Coarse Sand
VES7	1	2901.7	1.1	1.1	HA	Top Soil
	2	854.7	3.0	4.0		Fine Sand
	3	2541.7	17.2	21.2		Medium coarse sand
	4	4533.4				Coarse Sand

Nigerian Journal of Science and Environment 2025 Volume 23 (3) 20 – 44 ISSN: 3043 – 4440
https://doi.org/10.61448/njse233252

VES8	1	1744.3	1.2	1.2	HA	Top Soil
	2	506.7	3.8	5.0		Fine sand
	3	1506.9	29.9	34.9		Medium coarse Sand
	4	3960.7				Coarse Sand
VES9	1	2287.2	0.9	0.9	HA	Top Soil
	2	709.8	4.0	4.9		Fine Sand
	3	2282.8	18.3	23.2		Medium Coarse Sand
	4	2972.2				Coarse Sand

From Table 1, the lithological profiles across the study locations reveal a consistent subsurface sequence dominated by sandy formations. The lithology of the study area comprises of topsoil, fine sand, medium coarse sand, and coarse sand, with occasional occurrences of clayey sand. The prevalence of medium coarse and coarse sand horizons indicates significant groundwater storage and transmission potential, while the presence of clayey sand in some sections suggests localized semi-confining layers that may regulate vertical percolation and influence flow dynamics. These characteristics highlight a favorable hydrogeological framework for aquifer development and groundwater resource evaluation in the wetland area.

Tables 2 and 3 depict the Vertical Electrical Sounding (VES) survey at nine locations in Aviara wetland. It revealed key subsurface and aquifer characteristics.

TABLE 2: Computed Geo-Electric and Hydraulic Parameters of Aviara

VES NUMBER	**AQUIFER RESISTIVITY Ωm**	**AQUIFER THICKNESS h(m)**	**LONGITUDINAL CONDUCTANCE**	**AQUIFER TRANSVERSE RESISTANCE**	**AQUIFER TRANSMISSIVITY** m^2/day	**AQUIFER HYDRAULIC CONDUCTIVITY** m/day
VES 1	1430.8	22.9	0.1601	32765.32	174.04	7.6
VES 2	1140.8	17.0	0.1490	19393.6	129.2	7.6
VES 3	904.4	17.4	0.1924	15736.56	132.24	7.6
VES 4	1530.0	18.9	0.1235	28917	143.64	7.6
VES 5	1472.6	18.3	0.1243	26948.58	139.08	7.6
VES 6	2323.0	15.4	0.0663	35774.2	117.04	7.6
VES 7	2541.7	17.2	0.0677	43717.24	130.72	7.6
VES 8	1506.9	29.9	0.1984	45056.31	227.24	7.6

Nigerian Journal of Science and Environment 2025 Volume 23 (3) 20 – 44 ISSN: 3043 – 4440
https://doi.org/10.61448/njse233252

VES 9	2282.8	18.3	0.0802	41775.24	139.08	7.6

TABLE 3: Computed Geo-Electric and Hydraulic Parameters Of Aviara

VES Number	Electrical conductivity $\mu s/cm$	Pore water (Ωm)	Formation Factor	Porosity (%)
VES 1	34	294.12	5.193	0.439
VES 2	46	217.39	6.810	0.383
VES 3	17	588.24	5.038	0.446
VES 4	41	243.9	7.087	0.376
VES 5	32	312.5	5.678	0.420
VES 6	18	555.56	4.181	0.489
VES 7	30	333.33	8.542	0.342
VES 8	35	285.71	5.630	0.421
VES 9	19	526.32	4.092	0.494

As seen in tables 2 and 3, aquifer resistivity ranged from 904.4 Ωm to 2541.7 Ωm, reflecting a range from fine-grained moist sediments to coarse, resistive sands. Aquifer thickness varied between 15.4 m (VES 6) and 29.9 m (VES 8), with thicker zones indicating more saturated layers favorable for groundwater. Longitudinal conductance values ranging from 0.0663–0.1984 S suggested poor to moderate aquifer protection, with VES 3 and VES 8 showing relatively better protection. Transverse resistance ranged from 15,736.56 to 45,056.31 Ωm², while transmissivity values varied from 117.04 to 227.24 m²/day, identifying VES 8 as the most productive zone. Hydraulic conductivity was consistent at 7.6 m/day, aligning with regional data. Groundwater electrical conductivity ranged from 17 to 46 μS/cm, indicating fresh to moderately mineralized water. Formation factors ranged from 4.092 to 8.542 further support the presence of porous, well-connected sand units favorable for groundwater storage and movement. Porosity values ranged from 0.342 to 0.494 (%), indicating that the aquifer materials are predominantly sandy formations with high groundwater storage potential. The lower value (0.342) suggests moderately compacted sands with good water retention, while the higher value (0.494) corresponds to loose, fine to medium sands with very high pore space availability. These results confirm a prolific, high-yielding aquifer system, especially within deeper fine to medium coarse sand layers, suitable for sustained pumping and productive borehole development aligning with Atakpo (2009), who reported similar hydraulic conductivity values ranging 4.6–8.8 m/day for the Isoko South area. Zones with higher transmissivity are particularly suitable for productive boreholes. The results also align with Egbai *et al.*, (2015) who reported similar transmissivity values ranging from 161. m²/day to 251 m²/day.

Figure 8 presents the geoelectric section of Aviara, showing four distinct subsurface layers at each of the nine VES locations. In total, five lithologic units were delineated across the area, namely topsoil, fine sand, clayey sand, medium coarse sand, and coarse sand which together define the lithological framework and aquifer potential of the area.

Nigerian Journal of Science and Environment 2025 Volume 23 (3) 20 – 44 ISSN: 3043 – 4440
https://doi.org/10.61448/njse233252

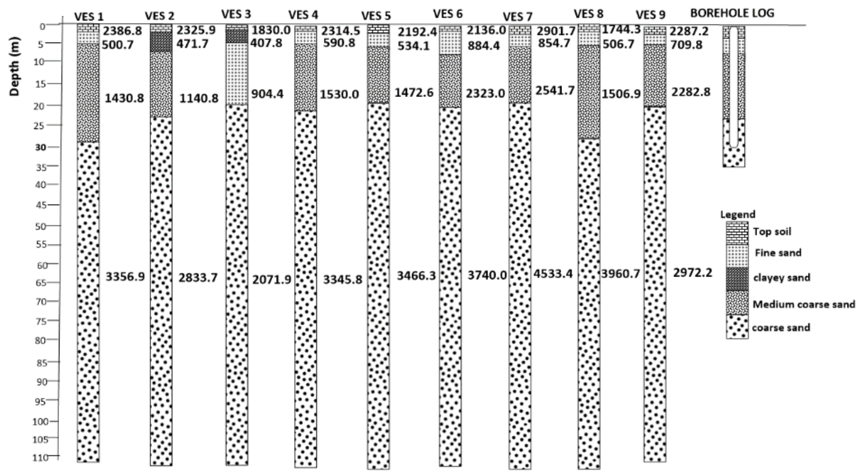

Figure 8: Geoelectric section of VES 1 – VES 9

The geoelectric sections in Figure 8 reveal a thin, resistive topsoil ranging from 1744.3 to 2901.7 Ωm. The second layer is mostly fine sand, ranging from 500.7 to 884.4 Ωm, except at VES 2 and 3, where lower-resistivity clayey sand ranging from 407.8 to 471.7 Ωm occurs. The main aquifer occurs in the third layer as medium to coarse sand, ranging from 1140.8 to 2541.7 Ωm at depths of 21.2 to 34.9 m, representing clean, highly permeable units consistent with productive aquifers, while VES 3 contains fine sand with a resistivity of 904.4 Ωm. The fourth layer is mainly coarse sand, but clayey sand at VES 2 and 3 may restrict groundwater flow. Borehole logs confirm a multi-layered aquifer system with spatial variations in lithology and resistivity, emphasizing the need for site-specific groundwater assessment. These findings are consistent with Egbai *et al.,* (2015), who also reported lateritic topsoil underlain by fine to medium sands and highlighted their significance as productive aquifer units in Idheze.

Figures 9 and 10 highlight the spatial distribution of aquifer resistivity at 5 m and 20 m depth across the study area, interpreted from geoelectric survey data respectively.

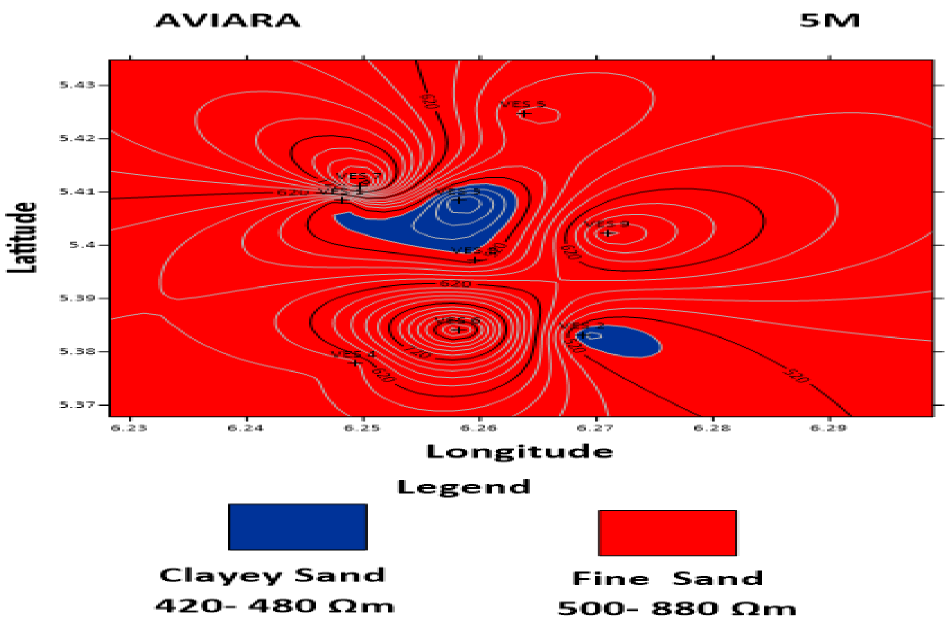

Figure 9: Aquifer Resistivity Map at 5 m depth of Aviara

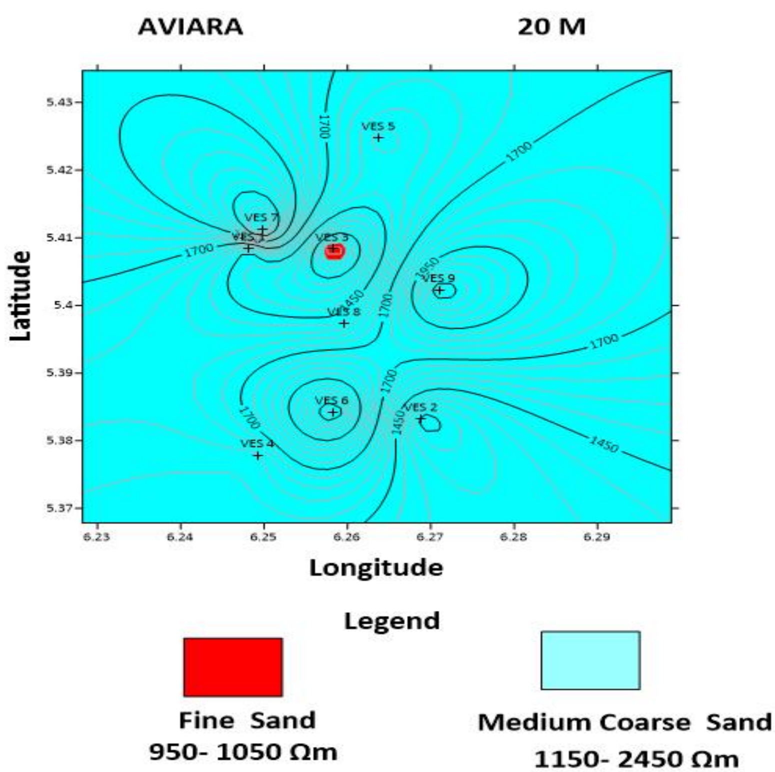

Figure 10: Aquifer Resistivity Map at 20 m depth of Aviara

As highlighted in figure 9, the aquifer resistivity map at 5 m depth of Aviara reveal clayey sand formation in VES 2 and VES 3 as seen in the blue color zone with resistivity value ranging from 420 Ωm to 480 Ωm while VES 1, VES 4, VES 5, VES 6, VES 7, VES 8, VES 9 indicate fine sand formation with resistivity value ranging from 500 Ωm to 880Ωm.

From figure 10, the aquifer resistivity map at 20 m depth in Aviara depicts fine sand at VES 3 with resistivity between 950 Ωm and 1050 Ωm, while VES 1, 2, 4, 5, 6, 7, 8, and 9 indicate medium coarse sand with higher resistivity values ranging from 1150 Ωm to 2450 Ωm. This suggests that this layer is more productive, capable of storing and transmitting larger volumes of groundwater.

Figures 11 and 12 highlight the spatial distribution of aquifer thickness and aquifer transmissivity across the study area, interpreted from geoelectric survey data.

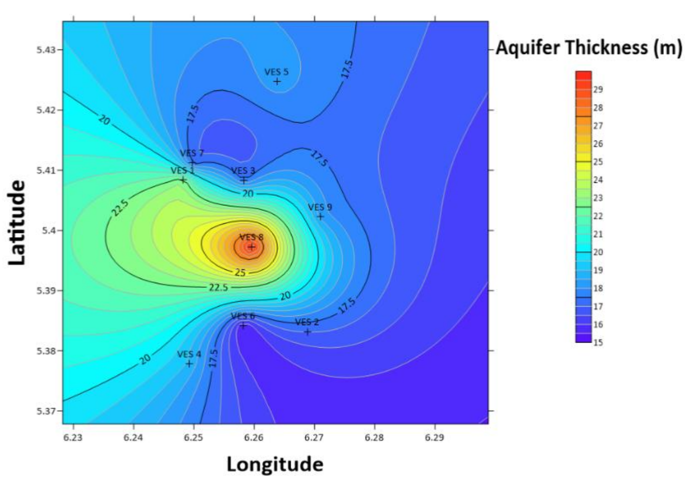

Figure 11: Aquifer Thickness Contour Map of Aviara

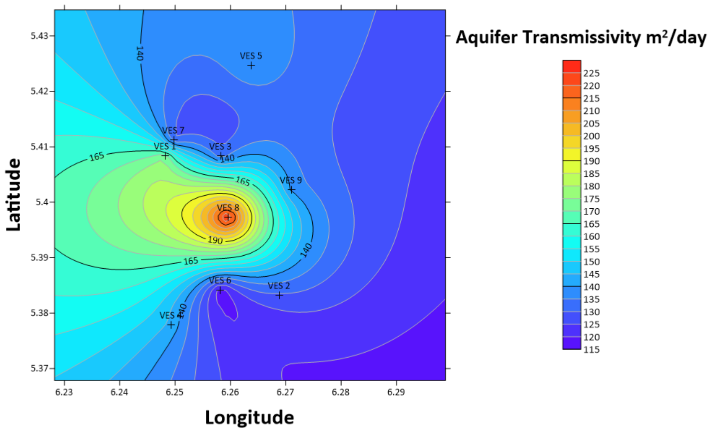

Figure 12: Aquifer Transmissivity contour map of Aviara

The aquifer thickness contour map in Figure 11 shows variations from 15 m to 29 m across Aviara. The thickest aquifer (29 m) occurs at VES 8, indicating high groundwater storage potential. Moderate thickness (20–25 m) is found near VES 1, VES 3, and VES 7, while thinner zones (15–20 m) appear near VES 4, VES 5, VES 6, and VES 9. VES 8 is thus the most promising site for groundwater development.

The transmissivity contour map, as seen in Figure 12, reveals that the highest transmissivity, up to 225 m²/day, occurs around VES 8, indicating a highly permeable and productive aquifer. Moderate values, ranging from 150 to 190 m²/day, are found near VES 1, VES 3, and VES 7, while lower transmissivity, ranging from 115 to 145 m²/day, occurs near VES 2, VES 4, VES 5, and VES 6. A sharp gradient around VES 8 suggests a localized high-yield zone influencing groundwater flow.

Figure 13 illustrates the spatial variation in longitudinal conductance across the study area, which is a key parameter for assessing the protective capacity of the overburden above the aquifer while figure 14 presents the spatial distribution of formation factor across the study area, a parameter used to infer the porosity and permeability of subsurface materials. By analyzing these values, insights into groundwater storage and flow potential can be understood

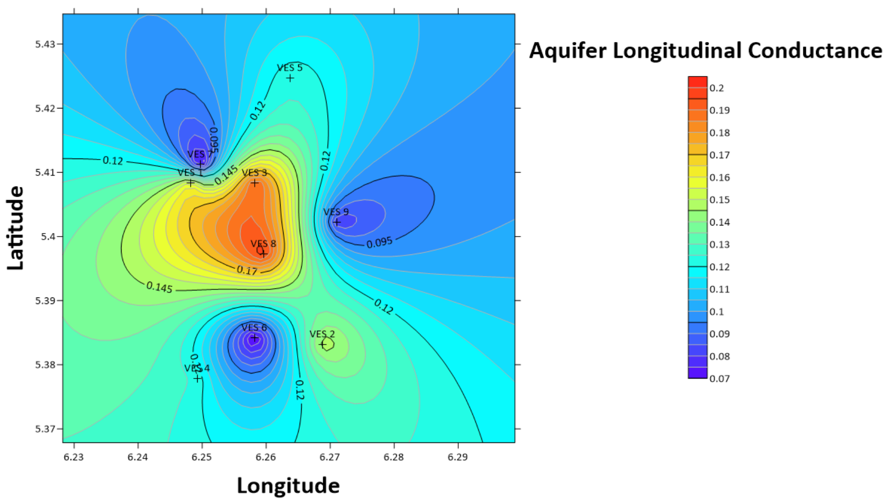

Figure 13: Longitudinal conductance contour map of Aviara

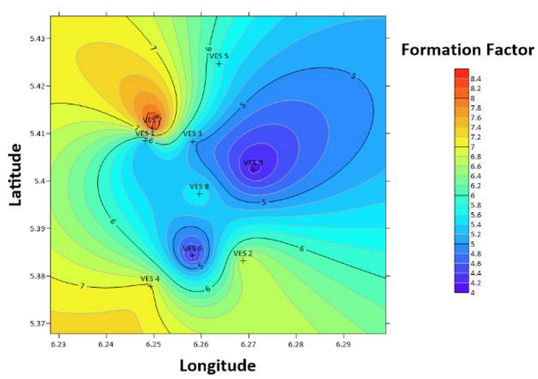

Figure 14: Formation Factor Contour Map of Aviara

The longitudinal conductance map in Figure 13 shows variations in aquifer protective capacity across Aviara. High conductance values up to 0.2 at VES 3 and VES 8 indicate excellent protection from thick, low-permeability layers. Moderate protection, ranging from 0.12 to 0.17, occurs near VES 1, VES 4, and between VES 2 and VES 5. Low protection, ranging from 0.07 to 0.11, is found at VES 6, VES 7, and VES 9, making these areas more prone to contamination. VES 3 and VES 8 are the most favorable for sustainable groundwater development.

As shown in Figure 14, the formation factor map illustrates subsurface porosity variations across the study area. Low formation factor values ranging from 4.0–4.8 around VES 6, and VES 9 indicate highly porous, sandy formations favorable for groundwater accumulation. In contrast, high values above values above 6.6 near VES 2, VES 4 and VES 7 suggest compact, less permeable materials with lower groundwater potential. Moderate values around VES 1, VES 3, VES 5, and VES 9 reflect mixed lithologies with average porosity and moderate aquifer potential

Electrical Resistivity Tomography and Induced Polarization

Nigerian Journal of Science and Environment 2025 Volume 23 (3) 20 – 44 ISSN: 3043 – 4440
https://doi.org/10.61448/njse233252

Figures 15, 16 and 17 represent the 2-D electrical resistivity tomography and IP model. It denotes both resistivity and IP heterogeneities within the subsurface. The resistivity results reveal four distinct subsurface layers with varying geoelectrical characteristics, each corresponding to different lithological units and hydrogeological significance respectively

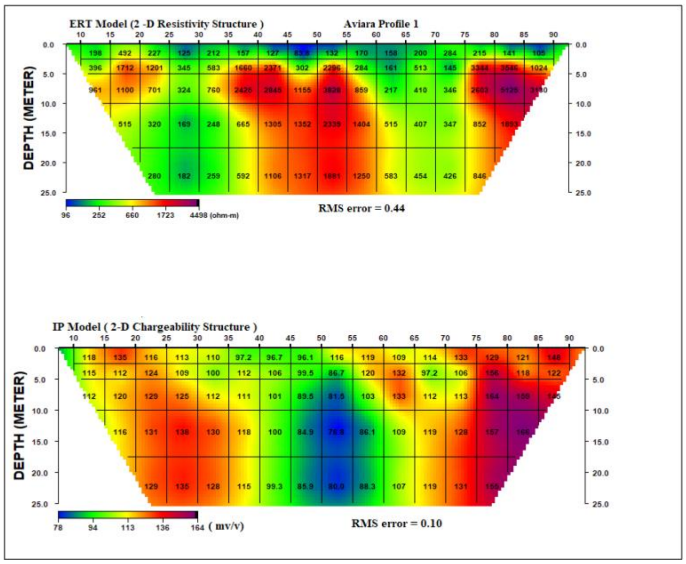

Fig.15: 2D distribution of electrical resistivity and induced polarization from profile 1 at Aviara

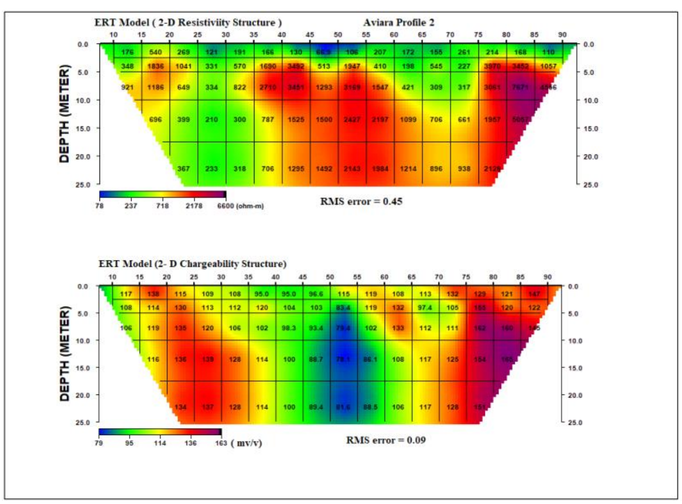

Fig.16: 2D distribution of electrical resistivity and induced polarization from profile 2 at Aviara

https://doi.org/10.61448/njse233252

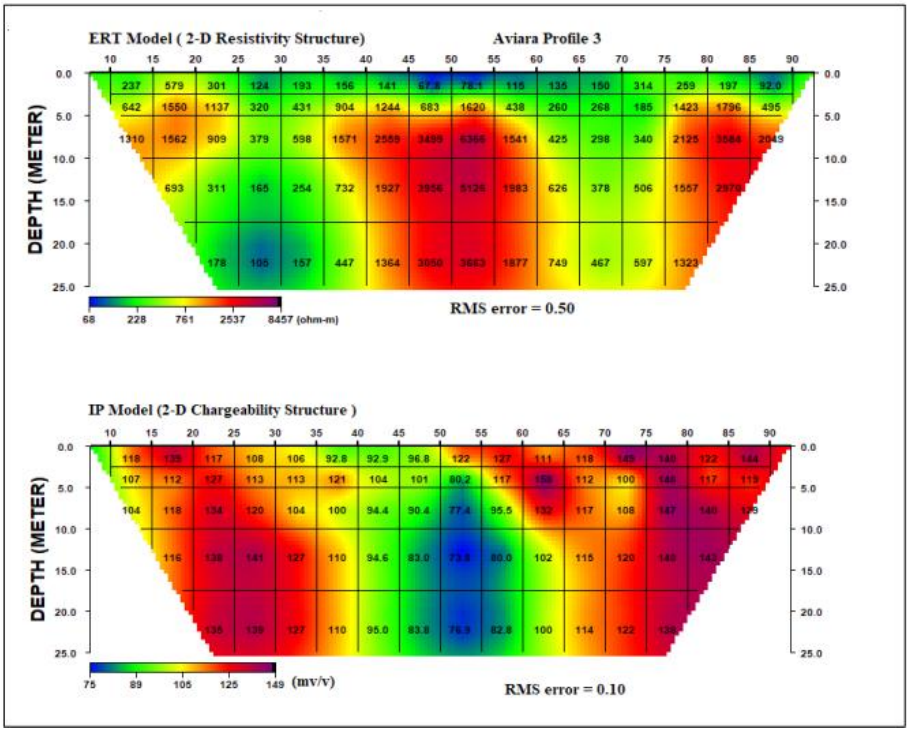

Fig.17: 2D distribution of electrical resistivity and induced polarization from profile 3 at Aviara

As denoted in Figure 15, Profile 1 reveals that the topsoil at a depth of 0–2 m exhibits low resistivity value ranging from 83.8–492 Ωm and high chargeability value ranging from 96.1–148 mV/V, indicating clay-rich, water-saturated material acting as a confining layer. The second layer at a depth of 2–10 m shows mixed resistivity ranging from 61–3628 Ωm with lower chargeability (<100 mV/V) in sandy zones and higher chargeability (>100 mV/V) in clayey sands, reflecting variable permeability. The third layer at a depth of 10–15.5 m features medium to coarse sand with resistivity value ranging from 169–2339 Ωm and generally low chargeability, consistent with a permeable aquifer. The fourth layer at a depth of 15.5–25 m shows high resistivity and low chargeability centrally, confirming coarse sands favorable for groundwater flow.

From figure 16, Profile 2 shows four subsurface layers based on geoelectric and Induced Polarization (IP) data. The top layer (0–2 m) has resistivity between 66.9 and 540 Ωm and high chargeability (95–147 mV/V), indicating clay-rich topsoil. Below, the second layer (2–10 m) has high resistivity (196–4856 Ωm) and chargeability ranging from 79.4 to 162 mV/V; lower chargeability (<100 mV/V) points to water-bearing fine sands, while higher values suggest clay. The third layer (10–15.5 m) shows resistivity of 210–5057 Ωm and chargeability patterns consistent with medium coarse sand aquifers where chargeability is low, and clayey sand where it is high. The fourth layer (15.5–25 m), especially in the center, has high resistivity and low chargeability, confirming coarse sand formation with good aquifer potential.

As observed in figure 17, Profile 3 identifies four subsurface layers using resistivity and chargeability data. The topsoil at a depth of 0–2 m has resistivity from 67.9 to 579 Ωm, ranging from clayey sand to sandy/drier soils. The second layer at a depth of 2–10 m shows resistivity between 185 and 6366 Ωm, indicating sandy formations with fine and coarse sands in high-resistivity zones. The third layer at a depth of 10–

Nigerian Journal of Science and Environment 2025 Volume 23 (3) 20 – 44 ISSN: 3043 – 4440
https://doi.org/10.61448/njse233252

15.5 m has resistivity from 165 to 5126 Ωm, suggesting medium coarse sand. The fourth layer at a depth of 15.5 -25 m varies from 105 to 3663 Ωm, with clayey sand on the low resistivity range and coarse sand in the high resistivity range. The 2-D IP model supports these results, showing high chargeability (> 100 mv/v) in clay-rich topsoil, variable chargeability in sandy layers (low values indicate good permeability), and low chargeability (<100 mv/v) in coarse sand zones with aquifer potential.

Hence, all the three profiles demonstrate that the wetland contains a protective surface clay layer underlain by multi-layered sandy aquifers of varying permeability, with the deeper coarse sand horizons providing the most reliable groundwater reserves. This geoelectrical and IP characterization not only enhances understanding of wetland aquifer dynamics but also provides a scientific basis for sustainable groundwater management, contamination risk assessment, and informed development planning in wetland communities. These results are broadly consistent with published ERT and IP studies in parts of Delta State. In particular, the presence of a shallow, low-resistivity and high-chargeability topsoil interpreted here as clay-rich and water-saturated agrees with regional investigations that report clayey near-surface overburden in Delta State (Emmanuel *et al.*, 2023, Otheremu *et al*., 2025)

Pumping Test

Figure 18 illustrates the results of the pumping test conducted to evaluate the aquifer's hydraulic properties, including transmissivity, hydraulic conductivity, and storativity. By analyzing the drawdown versus time data, information into the aquifer's capacity to transmit and store groundwater can be obtained

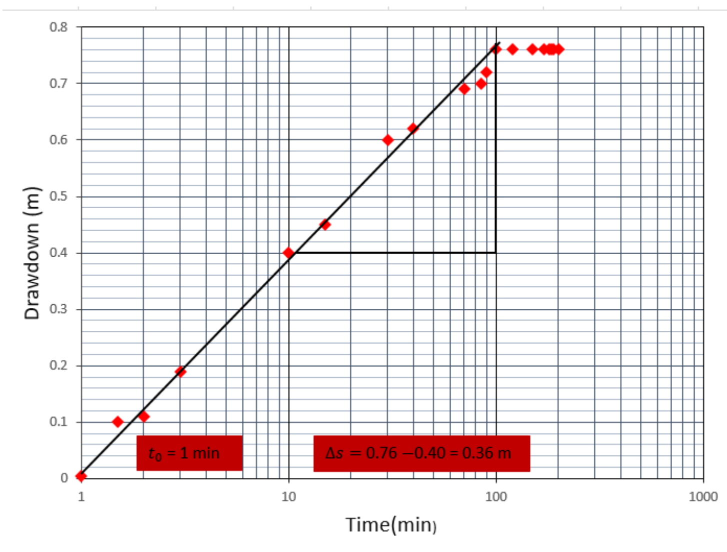

Figure.18: Graph of drawdown against time

Figure 18 shows a pumping test on a borehole with a discharge rate of 0.179 m³/min, well radius of 0.076 m, time of pumping t_0 = 1 min, and aquifer thickness of 17.2 m. The drawdown per log cycle was 0.36 m. These parameters were used in the Cooper-Jacob equation to calculate the aquifer transmissivity.

:

$$T = \frac{2.3\,Q}{4\pi \times \Delta S} = \frac{2.3 \times 0.179\, m^3/min}{4\pi \times 0.36\, m} = 0.091\, m^2/min = 131.04\ \ m^2/day$$

For specific capacity,

Sy = $\frac{Q}{\Delta S} = \frac{0.179}{0.36} = 0.497$ m²/min

For storativity,

$$S = \frac{2.3\,Tt_0}{r^2} = \frac{2.3 \times 0.091\, m^2/\,\text{min}\times 1\, min}{0.076^2\, m} = 36.24$$

Hydraulic conductivity, K:

$$K = \frac{T}{b} = \frac{0.091 m^2/min}{17.2\, m} = 0.0053\, m/min$$

Hence, converting the hydraulic conductivity to units of m/day,

$$K = 0.0053 \times 24 \times 60 = 7.6\, m/day$$

These results indicate that the aquifer possesses favorable hydrogeological properties capable of supporting sustainable groundwater development in the study area. They also suggest a moderate to high groundwater yield potential, with sufficient storage and transmissive capacity for domestic and agricultural uses. When compared with earlier pumping test studies in Delta State, the present results show close agreement. The transmissivity of 131.04 m²/day obtained in this study is slightly higher than the 96.48 m²/day reported by Ofomola *et al*., (2022) at Ozoro, while the hydraulic conductivity of 7.6 m/day is comparable to their 6.8 m/day**.** Similarly, the specific capacity of 0.497 m²/min exceeded that reported by Ofomola *et al*., (2022), which was 0.364 m²/min, suggesting somewhat greater productivity in the present study area. Hence, the comparable transmissivity, conductivity, and specific capacity values affirm the reliability of the present findings and confirm that the aquifers are moderately productive capable of supporting sustainable groundwater development in a wetland environment.

CONCLUSION

This study employed an integrated approach, combining Vertical Electrical Sounding (VES), Electrical Resistivity Tomography (ERT), and pumping test methods, to investigate the wetland aquifer systems of Aviara, Delta State. The geophysical results revealed a stratigraphy dominated by clay-rich topsoil, underlain by interbedded fine sands and clayey sands of variable resistivity and chargeability, with deeper medium to coarse sands identified as productive aquifers. These interpretations were reinforced by pumping test results, which provided key hydraulic parameters such as transmissivity and hydraulic conductivity, confirming the groundwater potential of the deeper sandy formations.

The integration of geophysical methods with Pumping test methods offers a robust framework for aquifer assessment and resource evaluation in wetland environments. The findings demonstrate significant groundwater potential in Aviara while underscoring the protective role of clay-rich overburden in reducing contamination risk. This approach is not only valuable for sustainable groundwater development and environmental protection in Aviara but also serves as a methodological model for similar wetland settings in the Niger Delta.

Statements and Declarations

Conflict of Interest

All authors have no conflict of interest to declare.

Funding

The authors did not receive support from any organization for the submitted work.

Competing Interests

The authors have no relevant financial or non-financial interests to disclose.

REFERENCES

Akpan, A. E., Ugbaja, A. N., and George, N. J. (2013). Integrated geophysical, geochemical and hydrogeological investigation of shallow groundwater resources in parts of the Ikom-Mamfe Embayment and the adjoining areas in Cross River State, Nigeria. *Environmental earth sciences*, *70*(3), 1435-1456

Amakiri, A. R. C., Amonieah, J., and Otugo, V. N. (2024). Estimation of electrical formation factor and porosity from VES for the aquifers in parts of Bayelsa state Nigeria. *International of multidisciplinary research and growth evaluation*, *5*, 480-487.

Anomohanran, O., and Iserhien-Emekeme, R. E. (2014). Estimation of aquifer parameters in Erho, Nigeria using the Cooper-Jacob evaluation method. *American Journal of Environmental Sciences*, *10*(5), 500.

Anomohanran, O., Oseme, J. I., Iserhien-Emekeme, R. E., and Ofomola, M. O. (2021). Determination of groundwater potential and aquifer hydraulic characteristics in Agbor, Nigeria using geo-electric, geophysical well logging and pumping test techniques. *Modeling Earth Systems and Environment*, *7*(3), 1639-1649.

Anomohanran, O., Nakireru, O. F., Ofomola, M. O., Anomohanran, E. E., and Abrika, E. O. (2023). Assessment of groundwater potential of Somebreiro-Warri plain sand of Ughelli, Nigeria. *Sustainable Water Resources Management*, *9*(1), 26.

Archie, G.E. (1942). The electrical resistivity logs as an aid in determining some reservoir characteristics. *Transaction of American Institute of Mining and Metallurgical Engineers, 146:54–62*

Atakpo, E. A. (2009). Groundwater and contaminant flow modeling in Olomoro area of Delta State. *Journal of the Nigerian Association of Mathematical Physics, (15): 205–212.*

Atakpo, EA and Akpoborie, AI (2011). Electrical Resistivity imaging of spilled crude at the Obuguru inter-tidal flat, Forcados area, Delta State, Nigeria. *Arch. Phys. Res. 2*(4), 166-175.

Azffri, S. L., Ibrahim, M. F., and Gödeke, S. H. (2022). Electrical resistivity tomography and induced polarization study for groundwater exploration in the agricultural development areas of Brunei Darussalam. *Environmental Earth Sciences*, *81*(8), 233.

Davidson, N. C. (2014). *How much wetland has the world lost? Long-term and recent trends in global wetland area. Marine and Freshwater Research*, 65, 936–941. https://doi.org/10.1071/MF14173

Diab, A. I., Sanuade, O., and Radwan, A. E. (2023). An integrated source rock potential, sequence stratigraphy, and petroleum geology of (Agbada-Akata) sediment succession, Niger delta: application of well logs aided by 3D seismic and basin modeling. *Journal of Petroleum Exploration and Production Technology*, *13*(1), 237-257.

Emmanuel, E. D., Doro, K. O., Iserhien-Emekeme, R. E., and Atakpo, E. A. (2023). Using geophysics to guide the selection of suitable sites for establishing sustainable earthen fishponds in the Niger-Delta region of Nigeria. *Heliyon*, *9*(6).

Egbai, J. C., Aigbogun, C. O., Iserhien-Emekeme, R. E., and Pius, E. (2015). Delineation of Aquifer Potential and Lithology from Geo-Electric Sounding in Idheze, Isoko North LGA of

Delta State. *Asian Journal of Applied Sciences*, *3*(1).

Eyankware, M. O., and Ephraim, B. E. (2021). A comprehensive review of water quality monitoring and assessment in Delta State, Southern Part of Nigeria. *Journal of Environmental & Earth Sciences*, *3*(1).

Gomo, M. (2019). On the interpretation of multi-well aquifer-pumping tests in confined porous aquifers using the Cooper and Jacob (1946) method. *Sustainable Water Resources Management*, *5*(2), 935-946.

Griffiths, LN and Mitsch, WJ (2020) Nutrient retention via sedimentation in a created urban stormwater treatment wetland. *Science of the Total Environment 727, 138337*

Jiao, J J; Rushton, K. R (1995). Sensitivity of drawdown to parameters and its influence on parameter estimation for pumping test in large diameter wells. Groundwater, 33 (5): 794-800.

Keddy, P.A. (2010). Wetland ecology: principles and conservation *(2nd ed.). New York: Cambridge University Press.* ISBN 978-0521519403

Kouadio, K. E., Abrakasa, S., Ikiensikimama, S. S., and Botwe, T. (2020). Source Rocks Characterization Of Agbada And Akata Formations In The Niger Delta, Nigeria. *European Journal of Environment and Earth Sciences*, *1*(4).

Kruseman, G. P., and De Ridder, N. A. (2000). Analysis and Evaluation of pumping test data second edition. *Published by International institute for land reclamation and improvement. 372p*.

Martinho, E. (2023). Electrical resistivity and induced polarization methods for environmental investigations: an overview. *Water, Air, & Soil Pollution*, *234*(4), 215.

Newton, A., Icely, J., Cristina, S., Perillo, G. M., Turner, R. E., Ashan, D., and Kuenzer, C. (2020). Anthropogenic, direct pressures on coastal wetlands. *Frontiers in Ecology and Evolution*, *8*, 144.

Nwankwoala, H. O; and Okujagu, D. C. (2014). A review of wetlands and coastal resources of the Niger Delta: potentials, challenges and prospects. *Environment. Ecosystem. Sci*, *5*, 37-46.

Ofomola, M. O., Ako, B. D., and Adelusi, A. O. (2016). Flow direction and velocity determination of dumpsite-induced groundwater contamination in part of Delta State, Nigeria. *Arabian Journal of Geosciences*, *9*, 1-12

Ofomola, M. O; Otheremu, O. P., Ohwoghere-Asuma, O., and Anomohanran, O. (2022). Determination of aquifer hydraulic characteristics from surface electrical and borehole measurements in Ozoro, Nigeria. *Nigerian Journal of Technological Development*, *19*(3), 240-249.

Ofomola, M. O., Abriku, E. O., Anomohanran, O., Otheremu, P. O., and Utieyin, B. S. (2023). Evaluation of geophysical parameters for groundwater productivity in the Commune of Jesse, Delta State Nigeria. *Nigerian Journal of Basic and Applied Sciences*, *31*(1), 85-93.

Okonkwo, C. N. P; Kumar, L., and Taylor, S (2015). The Niger Delta wetland ecosystem: What threatens it and why should we protect it? *African journal of environmental science and technology*, *9*(5), 451-463.

Otheremu, O. P., Ofomola, M. O., and Atakpo, E. A. (2025). Subsurface Lithology and Its Impact on Aquifer Characteristics to Support Sustainable Groundwater Development in Ibedeni, Delta State, Nigeria. *Journal of Applied Sciences and Environmental Management*, *29*(9), 2838–2847.

Sánchez-Higueredo, L. E., Ramos-Leal, J. A., Morán-Ramírez, J., Moreno-Casasola, P., Lithgow, D., de León, S. G., and Peralta-Pelaez, L. A. (2025). Wetland vegetation zoning as a response to groundwater complex systems. *Science of The Total Environment, 958, 177893.*

Sharma, L. K., and Naik, R. (2024). Wetland Ecosystems. In *Conservation of Saline Wetland Ecosystems: An Initiative towards UN Decade of Ecological Restoration* (pp. 3-32). Singapore: Springer Nature Singapore

Short, K.C.; Stauble, A. J. (1967).Outline of Geology of Niger Delta, Bull. AAPG .51(5):761- 779.

Vander Velpen, B.P.A. (2004). winResist version 1.0. M.Sc. Research project ITC, Daft, Netherland